Methods of Generating Multiple Uncorrelated Rayleigh Fading Processes

Cheng-Xiang Wang and Matthias Pätzold
Department of Information and Communication Technology
Faculty of Engineering and Science, Agder University College
Grooseveien 36, N-4876 Grimstad, Norway
E-mail: cheng.wang@hia.no

Abstract - **Simulating space-time-selective fading channels, multiple-input multiple-output (MIMO) channels, frequency-selective and diversity-combined fading channels often requires the generation of multiple uncorrelated Rayleigh fading waveforms. In this paper, it is shown how the deterministic channel modeling approach can be applied to simulate multiple Rayleigh fading processes correlated in time, but uncorrelated between processes. Two appropriate parameter computation methods are investigated to guarantee the uncorrelatedness between different simulated fading processes. Numerical results show that the resulting deterministic channel simulator can accurately reproduce all of the desired statistical properties of the reference model. Moreover, three different procedures are presented to enable the efficient generation of multiple sequences of Rayleigh fading processes uncorrelated in time and between sequences. These methods are useful for simulating perfect interleaving channels.**

I. Introduction

Computer simulation of multiple uncorrelated fading processes has become the subject of considerable research effort due to the increased interest in using smart antennas or multiple antennas to improve the reliability of wireless communication systems. Simulators which enable the accurate and efficient generation of multiple uncorrelated fading processes are therefore of theoretical and practical importance. As well as being useful for simulating general space-time-selective fading channels and multiple-input multiple-output (MIMO) channels, this capability is also desirable, for example, to simulate frequency-selective and diversity-combined fading channels.

Jakes' deterministic channel simulator [1] has widely been used for simulating time-correlated Rayleigh fading channels. However, it is difficult for Jake's simulator to create multiple uncorrelated fading waveforms. Different modifications of Jakes' simulator are therefore presented in [2–5], but they still retain some undesirable properties. In this paper, we apply the deterministic sum-of-sinusoids channel modeling approach [6–8] to simulate multiple uncorrelated Rayleigh fading processes by appropriately choosing the discrete Doppler frequencies. Its advantage over other forms of fading simulators in [1–5] lies in both accurate reproduction of all of the desired statistical properties of the reference model and efficient implementation due to the retained deterministic nature. Two parameter computation methods [8] are revisited concerning how to design the discrete Doppler frequencies in such a way that they are disjoint (mutually exclusive) for different simulated processes, which guarantees the uncorrelatedness between different processes.

For the simulation and performance evaluation of coded communication systems, it is sometimes also desirable to produce multiple sequences of Rayleigh fading processes uncorrelated in time and between sequences. The independent fading in different symbols is established by means of perfect interleaving/deinterleaving. In this case, the channel is considered as memoryless, and the output of the channel can be regarded as a sequence of independent and identically distributed (i.i.d.) random variables. In this paper, three modeling methods will be presented to enable the efficient generation of multiple uncorrelated i.i.d. Rayleigh sequences.

II. Generation of Multiple Uncorrelated Rayleigh Fading Processes

The confronted task at hand is to simulate multiple Rayleigh fading processes correlated in time, but uncorrelated between processes. Ideally, these Rayleigh processes should fulfill the following conditions: 1) The inphase and quadrature components of each underlying complex Gaussian random process are zero-mean independent Gaussian processes with identical variances and autocorrelation functions (ACFs); 2) the cross-correlation function (CCF) of any pair of Rayleigh processes must be zero.

Suppose now that the desired ℓth ($\ell = 1, 2, \ldots, \mathcal{L}$) Rayleigh fading process $\zeta_\ell(t)$ is given by

$$\zeta_\ell(t) = |\mu_\ell(t)| = |\mu_{1,\ell}(t) + j\mu_{2,\ell}(t)| \qquad (1)$$

where $\mu_\ell(t)$ is a zero-mean complex Gaussian random process, $\mu_{1,\ell}(t)$ and $\mu_{2,\ell}(t)$ are uncorrelated real Gaussian

0-7803-7757-5/03/$17.00 ©2003 IEEE

random processes with common variance σ_0^2. The amplitude probability density function (PDF) of $\zeta_\ell(t)$ is the following Rayleigh distribution

$$p_\zeta(x) = \frac{x}{\sigma_0^2}\exp(-\frac{x^2}{2\sigma_0^2}), \quad x \geq 0. \tag{2}$$

According to Clark's reference model [1, 9], the propagation environment is assumed to be two-dimensional isotropic scattering with an omnidirectional antenna at the receiver. In this case, the ACF of $\mu_{i,\ell}(t)$ $(i = 1, 2)$ is specified as

$$r_{\mu_{i,\ell}\mu_{i,\ell}}(\tau) = \sigma_0^2 J_0(2\pi f_{max}\tau) \tag{3}$$

where f_{max} is the maximum Doppler frequency and $J_0(\cdot)$ denotes the zeroth-order Bessel function of the first kind. As mentioned above, the CCF between the inphase and quadrature components of each complex Gaussian random process is zero, i.e., $r_{\mu_{1,\ell}\mu_{2,\ell}}(\tau) = 0$ holds for all $\ell = 1, 2, \ldots, \mathcal{L}$. Also, different complex Gaussian random processes $\mu_\ell(t)$ and $\mu_\lambda(t)$ are uncorrelated for $\ell \neq \lambda$ $(\ell, \lambda = 1, 2, \ldots, \mathcal{L})$, which indicates that $r_{\mu_\ell\mu_\lambda}(\tau) = 0$.

Based on the principle of deterministic channel modeling approach [8], the ℓth $(\ell = 1, 2, \ldots, \mathcal{L})$ Rayleigh fading process is modeled as

$$\tilde{\zeta}_\ell(t) = |\tilde{\mu}_\ell(t)| = |\tilde{\mu}_{1,\ell}(t) + j\tilde{\mu}_{2,\ell}(t)| \tag{4}$$

where

$$\tilde{\mu}_{i,\ell}(t) = \sum_{n=1}^{N_{i,\ell}} c_{i,n,\ell}\cos(2\pi f_{i,n,\ell}t + \theta_{i,n,\ell}), \quad i = 1, 2. \tag{5}$$

Here, $N_{i,\ell}$ defines the number of sinusoids, $c_{i,n,\ell}$, $f_{i,n,\ell}$, and $\theta_{i,n,\ell}$ are called the Doppler coefficients, the discrete Doppler frequencies and the Doppler phases, respectively. It is worth mentioning that all these parameters will be determined at the beginning of the simulation run and kept constant during simulation. Consequently, $\tilde{\mu}_{i,\ell}(t)$ is a deterministic function and the resulting channel simulator is of deterministic feature. The amplitude PDF $\tilde{p}_\zeta(x)$ of $\tilde{\zeta}_\ell(t)$ is computed by [8, 10]

$$\tilde{p}_\zeta(x) = x\int_0^{2\pi} \tilde{p}_{\mu_1}(x\cos\theta)\cdot\tilde{p}_{\mu_2}(x\sin\theta)\, d\theta \tag{6}$$

where

$$\tilde{p}_{\mu_i}(x) = 2\int_0^\infty \left[\prod_{n=1}^{N_{i,\ell}} J_0(2\pi c_{i,n,\ell}\nu)\right]\cos(2\pi\nu x)\, d\nu, \quad i = 1, 2. \tag{7}$$

The ACF of $\tilde{\mu}_{i,\ell}(t)$ is given by

$$\tilde{r}_{\mu_{i,\ell}\mu_{i,\ell}}(\tau) = \sum_{n=1}^{N_{i,\ell}} \frac{c_{i,n,\ell}^2}{2}\cos(2\pi f_{i,n,\ell}\tau). \tag{8}$$

It follows from [8] that the CCF of $\tilde{\mu}_{1,\ell}(t)$ and $\tilde{\mu}_{2,\ell}(t)$ can be written as $\tilde{r}_{\mu_{1,\ell}\mu_{2,\ell}}(\tau) = 0$ for all τ, if

$$f_{1,n,\ell} \neq \pm f_{2,m,\ell} \tag{9}$$

holds for all $n = 1, 2, \ldots, N_{1,\ell}$ and $m = 1, 2, \ldots, N_{2,\ell}$. By analogy, in order to ensure that the different processes $\tilde{\mu}_\ell(t)$ and $\tilde{\mu}_\lambda(t)$ are uncorrelated for $\ell \neq \lambda$, one merely has to design the Doppler frequencies $f_{i,n,\ell}$ in such a way that they are disjoint for different processes, i.e.,

$$f_{i,n,\ell} \neq \pm f_{j,m,\lambda}, \quad \ell \neq \lambda, \tag{10}$$

where $i, j = 1, 2$, $n = 1, 2, \ldots, N_{i,\ell}$, $m = 1, 2, \ldots, N_{j,\lambda}$, and $\ell, \lambda = 1, 2, \ldots, \mathcal{L}$. Subsequently, two parameter computation methods will be revisited concerning how to fulfill the conditions (9) and (10).

A. Method of Exact Doppler Spread (MEDS)

By using the MEDS [8], $\theta_{i,n,\ell}$ in (5) are the outcomes of a random generator uniformly distributed over $(0, 2\pi]$, while $c_{i,n,\ell}$ and $f_{i,n,\ell}$ are given by

$$c_{i,n,\ell} = \sigma_0\sqrt{\frac{2}{N_{i,\ell}}} \tag{11}$$

and

$$f_{i,n,\ell} = f_{max}\sin(\Phi_{i,n,\ell}) \tag{12}$$

respectively, where

$$\Phi_{i,n,\ell} = \frac{\pi}{2N_{i,\ell}}(n - \frac{1}{2}). \tag{13}$$

Since $1 \leq n \leq N_{i,\ell}$, it follows that $\frac{\pi}{4N_{i,\ell}} \leq \Phi_{i,n,\ell} \leq \frac{\pi(N_{i,\ell}-1/2)}{2N_{i,\ell}}$ holds. A looser range for $\Phi_{i,n,\ell}$ is $0 < \Phi_{i,n,\ell} < \pi/2$. Note that within this range, $f_{i,n,\ell}$ [see (12)] are monotonously increasing values over the interval $(0, f_{max})$ when n increases from 1 to $N_{i,\ell}$. Therefore, $f_{1,n,\ell} \neq -f_{2,m,\ell}$ and $f_{i,n,\ell} \neq -f_{j,m,\lambda}$ can always be satisfied. The condition (9) can be fulfilled if and only if $\Phi_{1,n,\ell} \neq \Phi_{2,m,\ell}$ holds, which results in

$$\frac{N_{1,\ell}}{N_{2,\ell}} \neq \frac{2n-1}{2m-1} \tag{14}$$

for all $n = 1, 2, \ldots, N_{1,\ell}$, $m = 1, 2, \ldots, N_{2,\ell}$, and $\ell = 1, 2, \ldots, \mathcal{L}$. Analogously,

$$\frac{N_{i,\ell}}{N_{j,\lambda}} \neq \frac{2n-1}{2m-1} \tag{15}$$

can guarantee that the inequality (10) is satisfied, where $i, j = 1, 2$, $n = 1, 2, \ldots, N_{i,\ell}$, $m = 1, 2, \ldots, N_{j,\lambda}$, and $\ell, \lambda = 1, 2, \ldots, \mathcal{L}$. From (14) and (15), it is clear that the ratio of $N_{1,\ell}$ to $N_{2,\ell}$ and the ratio of $N_{i,\ell}$ to $N_{j,\lambda}$

must be unequal to the ratio of two odd numbers. Consequently, there is at maximum one odd value allowed for all $N_{i,\ell}$ ($i = 1, 2$ and $\ell = 1, 2, \ldots, \mathcal{L}$). For simulating 2-by-2 ($\mathcal{L} = 4$) MIMO channels, a possible set of 8 values for $N_{i,\ell}$ is $\{8, 9, 10, 12, 16, 32, 64, 128\}$. Note that large values have to be chosen for $N_{i,\ell}$ when $\mathcal{L} > 4$. However, we can select $N_{i,\ell}$ in such a way that (9) and (10) are not fulfilled for only few pairs of (n, m). In this case, the cross-correlations of any pair of processes are so small that they can be neglected in practice. The CCF between $\tilde{\mu}_{i,\ell}(t)$ and $\tilde{\mu}_{j,\lambda}(t)$ ($i = j$ and $\ell = \lambda$ cannot hold at the same time) is [8]

$$\tilde{r}_{\mu_{i,\ell}\mu_{j,\lambda}}(\tau) = \sum_{n=1}^{N_{i,\ell}} \sum_{m=1}^{N_{j,\lambda}} \frac{c_{i,n,\ell} c_{j,m,\lambda}}{2} \cos(2\pi f_{j,m,\lambda}\tau + \theta_{j,m,\lambda} - \theta_{i,n,\ell}), \quad \text{if } f_{i,n,\ell} = f_{j,m,\lambda}. \tag{16}$$

Substituting (11) with $\sigma_0 = 1$ into (16), it is clear that the maximum value $\tilde{r}_{max}$ of the CCF is $\tilde{r}_{max} = N_{\mathrm{e}} c_{i,n,\ell} c_{j,m,\lambda}/2 = N_{\mathrm{e}}/\sqrt{N_{i,\ell} N_{j,\lambda}}$, where N_{e} defines the number of equal frequencies in the sets $\{f_{i,n,\ell}\}$ and $\{f_{j,m,\lambda}\}$. For example, to simulate a 12-path ($\mathcal{L} = 12$) frequency-selective channel, a set of 24 values for $N_{i,\ell}$ could be $\{8, 9, 11, 13, 16, 17, 18, 19, 22, 23, 25, 26, 28, 29, 31, 32, 34, 36, 37, 41, 43, 47, 51, 53\}$. It follows that the maximum cross-correlation between $\tilde{\mu}_{i,\ell}(t)$ and $\tilde{\mu}_{j,\lambda}(t)$ is $\tilde{r}_{max} = 0.1005$, which occurs when $N_{i,\ell} = 18$ and $N_{j,\lambda} = 22$. Here, $f_{i,n,\ell} = f_{j,m,\lambda}$ holds for two pairs of (n, m): (5, 6) and (14, 17). However, when $f_{i,n,\ell} = f_{j,m,\lambda}$ holds, we can further replace $f_{i,n,\ell}$ by $f_{i,n,\ell} + \varepsilon$, where ε is a very small random variable which guarantees that $f_{i,n,\ell} \neq f_{j,m,\lambda}$ and $f_{i,n-1,\ell} < f_{i,n,\ell} < f_{i,n+1,\ell}$ hold. The resulting new set $\{f_{i,n,\ell}\}$ will not degrade too much the performance of the channel simulator and can satisfy again the relations (9) and (10).

By making use of (11), it can be shown that (6) approaches the Rayleigh distribution (2) if $N_{i,\ell} \to \infty$ [10]. Substituting (11) and (12) in (8), it can also be shown that $\tilde{r}_{\mu_{i,\ell}\mu_{i,\ell}}(\tau)$ tends to $r_{\mu_{i,\ell}\mu_{i,\ell}}(\tau)$ as $N_{i,\ell} \to \infty$. However, for finite values of $N_{i,\ell}$, we can only write $\tilde{p}_\zeta(x) \approx p_\zeta(x)$ and $\tilde{r}_{\mu_{i,\ell}\mu_{i,\ell}}(\tau) \approx r_{\mu_{i,\ell}\mu_{i,\ell}}(\tau)$. Fig. 1 compares the Rayleigh distribution with an example of $\tilde{p}_\zeta(x)$ for $N_{1,\ell} = 9$ and $N_{2,\ell} = 10$. The corresponding simulated PDF of the fading envelope is also presented in the figure to validate the analytical result. It is clear that the approximation error is small with the given numbers of sinusoids. Fig. 2 shows the ACF $\tilde{r}_{\mu_{i,\ell}\mu_{i,\ell}}(\tau)$ with $N_{i,\ell} = 10$ and the CCF $\tilde{r}_{\mu_{1,\ell}\mu_{2,\ell}}(\tau)$ with $N_{1,\ell} = 9$ and $N_{2,\ell} = 10$ for one simulated fading process by using the MEDS. The corresponding ACF $r_{\mu_{i,\ell}\mu_{i,\ell}}(\tau)$ and the CCF $r_{\mu_{1,\ell}\mu_{2,\ell}}(\tau)$ of the reference model are also illustrated in the figure for reasons of comparison. For the CCF, $\tilde{r}_{\mu_{1,\ell}\mu_{2,\ell}}(\tau) = r_{\mu_{1,\ell}\mu_{2,\ell}}(\tau) = 0$ holds for all τ. For the ACF, $\tilde{r}_{\mu_{i,\ell}\mu_{i,\ell}}(\tau)$ matches almost perfectly the desired one $r_{\mu_{i,\ell}\mu_{i,\ell}}(\tau)$ if τ is within the interval $[0, N_{i,\ell}/(2f_{max})]$, which includes approximately $N_{i,\ell}$ zero-crossings of $r_{\mu_{i,\ell}\mu_{i,\ell}}(\tau)$. In case that $\tau > N_{i,\ell}/(2f_{max})$, $\tilde{r}_{\mu_{i,\ell}\mu_{i,\ell}}(\tau)$ and $r_{\mu_{i,\ell}\mu_{i,\ell}}(\tau)$ will diverge and never converge again. Let us use τ_{max} to define an appropriate time interval $[0, \tau_{max}]$ over which the approximation of the desired ACF $r_{\mu_{i,\ell}\mu_{i,\ell}}(\tau)$ is of interest. Then, the required number of sinusoids is given by $N_{i,\ell} \geq \lceil 2f_{max}\tau_{max} \rceil$, where $\lceil x \rceil$ denotes the smallest integer larger than or equal to x. In Fig. 2, for $N_{i,\ell} = 10$ and $f_{max} = 91$ Hz, the corresponding τ_{max} is $\tau_{max} = N_{i,\ell}/(2f_{max}) = 0.0549$ s. Two uncorrelated simulated fading envelopes by using the MEDS are impressively shown in Fig. 3. The numbers of sinusoids for the two processes are chosen as follows: $N_{1,1} = 9$, $N_{2,1} = 10$, $N_{1,2} = 8$, and $N_{2,2} = 12$.

B. L_p-Norm Method (LPNM)

For the LPNM [8], $c_{i,n,\ell}$ and $\theta_{i,n,\ell}$ in (5) are the same as those given for the MEDS, while $f_{i,n,\ell}$ are determined by minimizing the following error norm

$$E^{(p)} = \left\{ \frac{1}{\tau_{max}} \int_0^{\tau_{max}} |r_{\mu_{i,\ell}\mu_{i,\ell}}(\tau) - \tilde{r}_{\mu_{i,\ell}\mu_{i,\ell}}(\tau)|^p d\tau \right\}^{1/p}, \quad p = 1, 2, \ldots. \tag{17}$$

Then, an optimized set of discrete Doppler frequencies $f_{i,n,\ell}$ will be attained by applying a numerical optimization algorithm, e.g., the Fletcher-Powell algorithm [11]. Consequently, the ACF $\tilde{r}_{\mu_{i,\ell}\mu_{i,\ell}}(\tau)$ of the deterministic process $\tilde{\mu}_{i,\ell}(t)$ will be fitted closely to the given ACF $r_{\mu_{i,\ell}\mu_{i,\ell}}(\tau)$ of the stochastic process $\mu_{i,\ell}(t)$.

It is important to mention that the global minimum of $E^{(p)}$ cannot be guaranteed to be found by the Fletcher-Powell algorithm, like any other suitable optimization algorithm. In general, a local minimum of $E^{(p)}$ is obtained. The advantage we may take from this property is that various local minima lead to various disjoint sets of discrete Doppler frequencies $f_{i,n,\ell}$. Therefore, we can easily satisfy the inequalities (9) and (10) by taking any of the following four measures: 1) choosing the number of sinusoids $N_{i,\ell}$ such that the relations (14) and (15) are fulfilled, 2) minimizing (17) by using different values of p, 3) minimizing (17) with different values of τ_{max}, and 4) carrying out the optimization by using different starting values for $f_{i,n,\ell}$. The method of equal distances, the method of equal areas, and even the MEDS can, for example, be employed to get the starting values for $f_{i,n,\ell}$ [8].

Since the relation $c_{i,n,\ell} = \sigma_0\sqrt{2/N_{i,\ell}}$ applies for both the MEDS and the LPNM, the obtained amplitude PDF $\tilde{p}_\zeta(x)$ [see (6)] by using the LPNM will be identical to the result shown in Fig. 1 with the same parameters. In Fig. 4, the optimized ACF $\tilde{r}_{\mu_{i,\ell}\mu_{i,\ell}}(\tau)$ with $N_{i,\ell} = 10$ and the CCF $\tilde{r}_{\mu_{1,\ell}\mu_{2,\ell}}(\tau)$ with $N_{1,\ell} = N_{2,\ell} = 10$ are demonstrated in comparison with the reference ACF $r_{\mu_{i,\ell}\mu_{i,\ell}}(\tau)$ and CCF $r_{\mu_{1,\ell}\mu_{2,\ell}}(\tau)$, respectively. As starting values for the discrete Doppler frequencies $f_{i,n,\ell}$, the expression (12) determined by the MEDS has been used. The upper limit for

the integral in (16) is still given by $\tau_{max} = 0.0549$ s. The optimization of the ACF $\tilde{r}_{\mu_{i,\ell}\mu_{i,\ell}}(\tau)$ is based on the error norm $E^{(p)}$ with $p = 2$. The disjoint sets of $f_{1,n,\ell}$ and $f_{2,n,\ell}$ for the calculation of the CCF $\tilde{r}_{\mu_{1,\ell}\mu_{2,\ell}}(\tau)$ are ensured by using $p = 1$ and $p = 2$, respectively. Apparently, there is no cross-correlation between the deterministic processes $\tilde{\mu}_{1,\ell}(t)$ and $\tilde{\mu}_{2,\ell}(t)$, i.e., $\tilde{r}_{\mu_{1,\ell}\mu_{2,\ell}}(\tau) = r_{\mu_{1,\ell}\mu_{2,\ell}}(\tau) = 0$ holds for all τ. We observe that the ACF $\tilde{r}_{\mu_{i,\ell}\mu_{i,\ell}}(\tau)$ nearly coincides with the desired $r_{\mu_{i,\ell}\mu_{i,\ell}}(\tau)$ when τ is located in the interval $[0, \tau_{max}]$. Compared with the MEDS, only a slight improvement is achieved by using the LPNM.

III. Generation of Multiple Uncorrelated i.i.d. Rayleigh Sequences

In this section, three different methods will be presented to model efficiently multiple uncorrelated i.i.d. Rayleigh sequences.

A. Method of Sampled Processes (MSP)

One straightforward method is to directly use the randomly sampled versions of the above time-correlated fading processes by assuming that t is a uniformly distributed random variable in (4). Ideally, the finite-length sampled sequence will have the same PDF as a sampled version of the continuous-time signal. However, the simulating time T_{sim} should be sufficiently long and a sufficient number of samples must be ensured in the simulation. By using the MSP, the resulting sequence with 500000 samples are obtained from a fading process $\tilde{\zeta}(t)$ with $\sigma_0^2 = 1$, $f_{max} = 91$ Hz, $N_{1,\ell} = 9$, and $N_{2,\ell} = 10$, where t ranges from 0 to 60 s. The histogram for the amplitude is then calculated. The normalized histogram and the theoretical amplitude PDF are plotted in Fig. 5. A good agreement between the two PDFs is observed.

B. Equation Transformation Method (ETM)

Another method is the so-called ETM. It is well known that a Rayleigh distributed sequence is formed by taking the magnitude of a zero-mean complex Gaussian random sequence, the inphase and quadrature parts of which are i.i.d. It follows that the amplitude of the underlying complex Gaussian random sequence is Rayleigh distributed and the phase is uniformly distributed over $(0, 2\pi]$. A Rayleigh distributed random variable r can be obtained from a uniformly distributed random variable $u \in (0, 1]$ through the following transformation [12]

$$r = \sigma_0\sqrt{-2\ln u}\,. \tag{18}$$

Then, according to [13], a complex Gaussian distributed random variable μ can be constructed by using four independent uniformly distributed random variables $u_i \in (0, 1]$, $i = 1, 2, 3, 4$,

$$\mu = \mu_I + j\mu_Q = \sigma_0\sqrt{-2\ln u_1}\cos(2\pi u_3) + j\sigma_0\sqrt{-2\ln u_2}\sin(2\pi u_4)\,. \tag{19}$$

Using different seeds to generate different u_i can easily guarantee the condition of i.i.d. The simulated amplitude PDF by using the ETM is also shown in Fig. 5, where 500000 samples are again used. Obviously, the quality of the approximation to the Rayleigh distribution is slightly better for the ETM than for the MSP.

C. RANDN Method (RANDNM)

The last method is to directly use the MATLAB function *randn* for generating a real Gaussian distributed random sequence. Consequently, a Rayleigh sequence can be obtained by taking the absolute value of a complex Gaussian sequence: $\zeta = |\sigma_0 * randn(1, N) + j * \sigma_0 * randn(1, N)|$, where N represents the number of samples. Due to the simplicity, this method is widely employed by many researchers, e.g., in [14]. Fig. 5 also includes the simulated amplitude PDF by using the RANDNM, where $N = 500000$ Monto Carlo trials have been carried out. The excellent approximation accuracy to the Rayleigh PDF is observed.

IV. Conclusion

Altogether, two methods are presented to generate multiple uncorrelated Rayleigh fading processes, and three methods are provided to produce multiple uncorrelated i.i.d. Rayleigh sequences. These methods are expected to be useful for the modeling of MIMO, space-time-selective, frequency-selective, and diversity-combined multi-path fading channels.

Compared with the MEDS, the LPNM has slightly better performance but higher numerical computation expenditure. In order to guarantee the uncorrelatedness between different simulated fading processes, the LPNM is a more flexible method than the MEDS. In both cases, the statistical properties of the simulated processes match very closely the desired properties of the reference model.

For modeling i.i.d. Rayleigh sequences, it turns out that the ETM and the RANDNM outperform the MSP, which has high realization expenditure and therefore takes a lot of simulation time. Due to the simplicity, the RANDNM is strongly recommended.

References

[1] W.C. Jakes, Ed., *Microwave Mobile Communications*. New Jersey: IEEE Press, 1994.

[2] P. Dent, G.E. Bottomley, and T. Croft, "Jakes fading model revisited," *Electron. Lett.*, vol. 29, no. 13, pp. 1162–1163, June 1993.

[3] Y.X. Li and X. Huang, "The generation of independent Rayleigh faders," *Proc. IEEE ICC'00*, New Orleans, LA, USA, June 18–22, 2000, pp. 41–45.

[4] Y.B. Li and Y.L. Guan, "Modified Jakes model for simulating multiple uncorrelated fading waveforms," *Proc. IEEE ICC'00*, New Orleans, LA, USA, June 18–22, 2000, pp. 46–49.

[5] Y.R. Zheng and C.S. Xiao, "Improved models for the generation of multiple uncorrelated Rayleigh fading waveforms," *IEEE Commun. Lett.*, vol. 6, no. 6, pp. 256–258, June 2002.
[6] S.O. Rice, "Mathematical analysis of random noise," *Bell Syst. Tech. J.*, vol. 23, pp. 282–332, July 1944.
[7] S.O. Rice, "Mathematical analysis of random noise," *Bell Syst. Tech. J.*, vol. 24, pp. 46–156, Jan. 1945.
[8] M. Pätzold, *Mobile Fading Channels*. Chichester: John Wiley & Sons, 2002.
[9] R.H. Clarke, "A statistical theory of mobile-radio reception," *Bell Syst. Tech. J.*, vol. 47, pp. 957–1000, July/Aug. 1968.
[10] M. Pätzold, U. Killat, F. Laue, and Y. Li, "On the statistical properties of deterministic simulation models for mobile fading channels," *IEEE Trans. Veh. Technol.*, vol. 47, no. 1, pp. 254–269, Feb. 1998.
[11] R. Fletcher and M.J.D. Powell, "A rapidly convergent descent method for minimization," *Computer Journal*, vol. 6, no. 2, pp. 163–168, 1963.
[12] G.E. Johnson, "Constructions of particular random processes," *Proc. of the IEEE*, vol. 82, no. 2, pp. 270–285, Feb. 1994.
[13] A. Papoulis and S.U. Pillai, *Probability, Random Variables, and Stochastic Processes*. New York: McGraw-Hill, 2002.
[14] V. Tarokh, N. Seshadri, and A.R. Calderbank, "Space-time codes for high data rate wireless communication: performance criterion and code construction," *IEEE Trans. Inform. Theory*, vol. 44, no. 2, pp. 744–765, Mar. 1998.

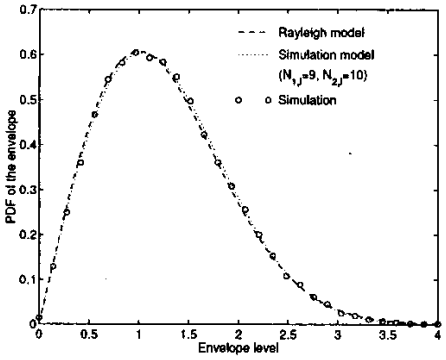

Fig. 1. The envelope PDFs of the Rayleigh model and the simulation model by using the MEDS ($\sigma_0^2 = 1$, $f_{max} = 91$ Hz).

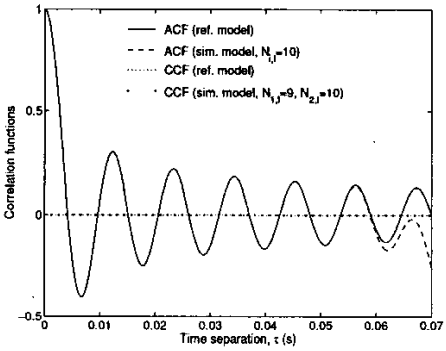

Fig. 2. Correlation functions of the reference model and the simulation model by using the MEDS ($\sigma_0^2 = 1$, $f_{max} = 91$ Hz).

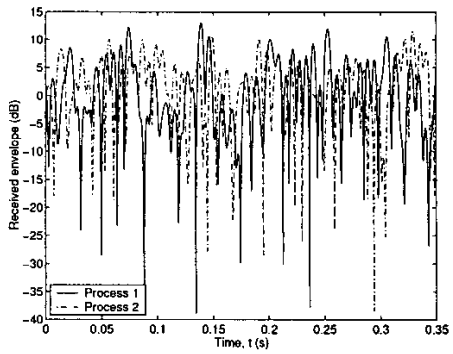

Fig. 3. Uncorrelated simulated fading envelopes by using the MEDS ($\sigma_0^2 = 1$, $f_{max} = 91$ Hz, $N_{1,1} = 9$, $N_{2,1} = 10$, $N_{1,2} = 8$, $N_{2,2} = 12$).

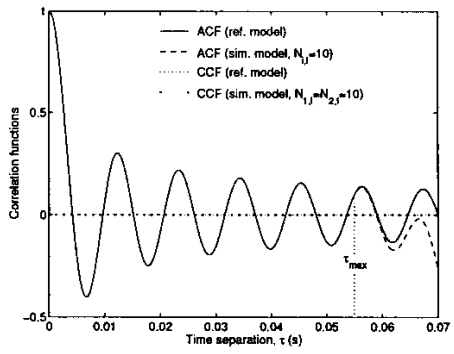

Fig. 4. Correlation functions of the reference model and the simulation model by using the LPNM ($\sigma_0^2 = 1$, $f_{max} = 91$ Hz).

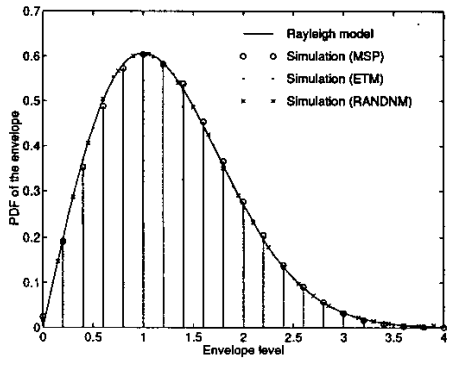

Fig. 5. The PDFs of the Rayleigh envelope and the simulated fading envelopes by using the MSP, the ETM, and the RANDNM ($\sigma_0^2 = 1$).